Single cell tracing reveals heterogeneous drug-, dose-, and time-dependent effects on cancer cell fates

Sean M. Gross, Crystal Sanchez-Aguila, Paulina J. Zhan, and Laura M. Heiser*

Department of Biomedical Engineering, OHSU Center for Spatial Systems Biomedicine, Knight Cancer Institute

Oregon Health & Science University, Portland, Oregon

*Lead Contact:

Laura M. Heiser

Department of Biomedical Engineering

2730 S. Moody Ave. CL3G

Portland, OR 97201

Email: heiserl@ohsu.edu

Key words: cell cycle, live-cell imaging, dose response, single cell, cancer

ABSTRACT

Understanding the molecular basis for drug-induced changes in cellular responses is critical for the identification of effective cancer treatments. Measurement of endpoint viability across a range of drug doses is the standard approach to quantify drug efficacy. While informative, this read-out does not account for the multiple cell fate decisions individual cancer cells undergo in response to drug treatment. As a consequence, the basis for drug-induced changes in cell numbers remains poorly defined. To evaluate the impact of cancer drugs on individual cells, we engineered AU565 breast cancer cells to express a fluorescent cell cycle reporter and then assessed dynamic responses to a panel of drugs. Detailed population and single cell analyses revealed heterogeneous drug-, dose-, and time-dependent effects on cell cycle durations and cell fates. Lapatinib induced dose-dependent extension of G1 duration and limited apoptosis. In contrast, cell fate responses varied with gemcitabine dose: low gemcitabine doses induced extension of S-G2 durations, whereas high doses induced apoptosis after prolonged exposure. Lastly, paclitaxel induced apoptosis and caused only modest cell cycle effects. Overall, our analyses revealed that each drug induced distinct impacts on cell fate that were dependent on the dose and duration of treatment. Understanding these differences has implications for the mechanisms of therapeutic resistance and the identification of effective drug combinations and treatment schedules.

INTRODUCTION

Drug dose response experiments are a workhorse of cancer cell biology(1-4). The standard dose response protocol involves counting the number of cells 72 hours after drug treatment and assuming exponential population growth that varies with drug dose. While this approach provides insights into cell viability, it does not take into account that final cell counts reflect a population of individual cells that have proceeded through repeated cell cycle check points and cell fate decisions(5-9). Drug effects may also be influenced by cell-to-cell variation, differ between doses, or dynamically evolve over time. Therefore, a detailed understanding of the influence of drugs on cell fate decisions may provide insights into the underlying processes by which drugs modulate cell viability.

To test the hypothesis that chemotherapeutic drugs act through distinct cell fate routes to alter cell numbers in a drug-, dose-, and time-dependent manner, we used live-cell imaging to systematically examine the responses of cells engineered to express a cell cycle reporter. Across drugs, we observed distinct routes to similar final cell numbers, often with dynamic effects that varied between cells and doses. These studies reveal the complexity of single-cell behavior underlying drug responses, provide mechanistic insights, and inform rational drug combinations.

RESULTS AND DISCUSSION

Drug responses induce dynamic changes in cell number and cell cycle phasing

To track drug responses in individual cells, we genetically transformed HER2+ AU565 breast cancer cells to stably express the HDHB cell cycle reporter(10) and a nuclear-localized red fluorescent protein (Fig. 1A,B). We then treated cells with escalating doses of five drugs commonly used to treat breast cancer (Fig. 1C), imaged cells every 30 minutes for 96H, and quantified cell cycle phase and total cell numbers.

We found that each drug effectively reduced cell numbers in a dose-dependent manner (Fig. 2A). Paclitaxel, gemcitabine, and doxorubicin led to cytotoxic effects in which the final cell numbers were below the starting cell numbers (Fig. 2A). In contrast, at the highest doses of palbociclib and lapatinib, the final cell numbers were approximately equal to the starting cell numbers, indicating cytostatic effects. For each drug, the pattern of cell counts varied across time, and moreover at high doses tended to trend lower as the duration of drug exposure increased--an effect that was most marked for gemcitabine. These data reveal the importance of considering the interaction between dose and duration when assessing drug responses (Fig. 2B) (5,6).

Next we sought to identify whether changes in cell numbers resulted from modulation of cell cycle phasing. Analyses of cell cycle activity revealed drug-, dose-, and time-dependent changes in the fraction of S-G2 cells (Fig. 2C,D). Lapatinib and palbociclib reduced the fraction of cells in S-G2 phase in a dose-dependent manner, whereas gemcitabine and doxorubicin increased this fraction. Interestingly, intermediate doses of lapatinib (50 nM) and paclitaxel (3 nM) induced biphasic responses, with an initial S-G2 reduction near 30H, followed by a second S-G2 reduction at 84H. This indicates that drug induced modulation of the cell cycle influences cell numbers across time.

Cancer therapies utilize distinct routes to achieve similar final cell counts

To explore the relationship between cell cycle and cell counts, we manually tracked cell lineages and deeply analyzed responses to three drugs that induced unique cell number and cell cycle profiles: lapatinib, gemcitabine, and paclitaxel (Fig. 3A). This approach revealed drug-

specific modulation of cell cycle phase and apoptosis. We found that the predominant effect of lapatinib was to increase the fraction of cells that failed to undergo a second division (Fig. 3B) by extending G1 durations (Fig. 3C). Lapatinib had modest impacts on cell death and S-G2 duration across doses (Fig. 3B, 3G). Notably, the dose dependent increases in G1 durations were accompanied by a widening of the G1 distribution, indicating that cells varied in their responsiveness to lapatinib, and that responsiveness did not equivalently increase with higher doses (Fig. 3C).

To understand the cyclical changes in cell cycle phasing from 50 nM lapatinib (Fig. 2C), we examined the various changes to cell cycle activity and found a reduction in the fraction of cells undergoing their first division beginning at 12H (Fig. 3F) coupled with an increase in the subsequent G1 duration following cell division (Fig. 3C). Together, these observations can explain the cell cycle synchronization observed in Figure 2: at the start of the assay, cells in G1 become delayed in their time to division, while cells in S-G2 become delayed in the onset of G1 following division. In summary, lapatinib primarily altered cell counts by extending G1 durations in a dose- and time-dependent manner.

In contrast to lapatinib, the effects of gemcitabine were not equivalent across doses or time. At low gemcitabine doses, cell numbers were primarily reduced due to increased S-G2 durations (Fig. 3D). At higher doses, cell numbers were reduced due to a combination of increased S-G2 durations and cell death (Fig. 3G). Quantification of cell death from gemcitabine revealed that most cells died during S-G2 phase (Fig.3H). Additionally, cell death was limited during the first 48H but increased markedly for the remainder of the experiment (Fig. 3E). This delayed onset of cell death can explain the time-dependent gemcitabine effects in the population-level cell counts (Fig. 2B).

Lastly, we evaluated the cell fate mechanisms underlying paclitaxel treatment. At 2 nM paclitaxel there were only modest changes in G1 or S-G2 durations. Instead, we observed a large number of apoptotic events, especially as compared to drugs that induced similar changes in cell numbers (Fig. 3G). Thus, paclitaxel primarily reduced cell numbers through apoptosis, in contrast to lapatinib and gemcitabine which also impacted cell cycle durations.

In summary, lapatinib, gemcitabine, and paclitaxel each modulated cell numbers through distinct cell fate routes and with different temporal dynamics. Our results indicate that typical dose response experiments obscure the effects that chemotherapeutic agents have on cell cycle progression and apoptosis. By revealing how these drugs uniquely impact cell fate at the single-cell level, our analyses have implications for how different cancer drugs may be combined to maximize therapeutic impact. For example, by suggesting particular drug combinations that modulate cell cycle effects in orthogonal ways, or by suggesting drug schedules that take advantage of the shift in cell cycle state of the overall population. Additionally, the observed variation in responsiveness between cells suggests that combining drugs that act through independent mechanisms provides two shots on the same cell that could maximize treatment efficacy. In summary, these studies provide a roadmap for understanding how cancer cells evade treatment and how drugs may be combined and timed for maximal effect.

ACKNOWLEDGEMENTS
These studies were supported by NIH research grants 1U54CA209988, U54-HG008100, Prospect Creek Foundation, Jayne Koskinas Ted Giovanis Foundation for Health and Policy, and Breast Cancer Research Foundation.

METHODS

Creation of stable cell lines

AU565 cells (ATCC CRL 2351), were grown in DMEM supplemented with 10% FBS. The coding fragment for clover-HDHB was cloned in frame into a transposase expression plasmid modified to also express a nuclear localized mCherry(11). Stable cell lines were created as previously described (11), and selected for 7 days with 0.75 µg/ml puromycin.

Drug dose response protocol

AU565 cells were plated at a density of 25,000 cells per well into 24-well Falcon plates (Corning #353047). 24H after plating the media was exchanged with Fluorobrite media supplemented with 10% FBS, glutamine, and penicillin-streptomycin. Cells were then treated with dose-escalation: Lapatinib (Selleckchem #S1028), gemcitabine (#S1149), paclitaxel (#S1150), doxorubicin (#S1208), and palbociclib (#S1116). After drug addition, the plates were imaged every 30 minutes for 96 hours using phase, GFP, and RFP imaging channels with the IncuCyte S3. At 48 hours, the media was replaced, and fresh media and drug were added. Four equally spaced image locations per well and three biological replicates were collected.

Automated Analyses

Phase, GFP, and RFP images were overlaid and collated into single files using FIJI (12), then segmented into three classes (nuclei, background, debris) using a trained classifier in Ilastik(13). The Ilastic segmented images and IncuCyte GFP images were used to count nuclei and determine cell cycle phase with Cell Profiler(14).

Manual Analyses

To manually track cells, GFP image sequences were registered using the FIJI plug-in 'StackReg'. Individual cells present in the first image and their progeny were followed to identify the time of G1 transition, apoptosis, and cell division using the plug-in mTrackJ(15). We excluded cells that were binucleated, had abnormally large nuclei, or were near the image border where complete lineages could not be tracked. The G1 transition was defined as the last frame before the nuclear intensity of the cell cycle reporter was below the level of the cytoplasm.

FIGURE LEGENDS

Figure 1. A. Schematic of expression plasmid with a bidirectional promoter driving expression of human DNA Helicase B (HDHB) fused to the green fluorescent protein clover, and a second transcript coding for NLS-RFP-NLS, a ribosome skipping domain (T2A), and a puromycin resistance protein. B. Quantification of nuclear intensity of the cell cycle reporter in a cell and its progeny across time. The time of G1/S transition and mitosis are demarcated with black and gray circle respectively. C. Schematic of the five drugs tested and the cell cycle phase they target.

Figure 2. Population responses to drugs vary with dose, time, and cell cycle. A. Average growth curves of AU565 cells tracked every 30 min for 96hr across an 8-point dose response for lapatinib, gemcitabine, paclitaxel, palbociclib, and doxorubicin. The null dose is colored red. Line traces show the average from three independent experiments. The black triangle at 48H indicates the addition of fresh drug and media. **B.** Dose response curves using the relative cell numbers at 48, 72, and 96H. **C.** Percentage of cells in S/G2 phase of the cell cycle across doses. 50 nM Lapatinib and 3 nM paclitaxel are colored blue. **D.** GFP images after 39.5H treatment with the indicated drug dose.

Figure 3. Responses of individual cells reveal molecular mechanisms that vary between drugs. A. Lineage trees of 25 lineages across 96H for various drug treatments. Tracks are colored coded based on cell cycle phase: gray indicates G1 and red indicates S/G2 phase. Track splitting indicates mitosis, and track ending prior to 96H corresponds to apoptosis. **B.** Quantification of cell outcomes (division, apoptosis, still present at end of experiment) for cells from the first and second generations treated with lapatinib, gemcitabine, or paclitaxel. **C.** Distributions of G1 durations for cells that underwent one division. **D.** Distributions of S-G2 durations. **E.** Accumulated cell death across time, normalized per 100 lineages. **F.** Time to first division for cells in the CTRL condition (red line) compared to 50 nM lapatinib (gray line). **G.** Cell count relative to 0H against cell death per lineage. **H.** Cell death counts per 100 lineages after 96H and the percentage of cells that died in G1 compared to S/G2 for 250nM lapatinib, 30 nM gemcitabine, 3 nM paclitaxel.

REFERENCES

1. Barretina J*, et al.* (2012) The Cancer Cell Line Encyclopedia enables predictive modelling of anticancer drug sensitivity. *Nature* 483(7391):603-607.
2. Garnett MJ*, et al.* (2012) Systematic identification of genomic markers of drug sensitivity in cancer cells. *Nature* 483(7391):570-575.
3. Heiser LM*, et al.* (2012) Subtype and pathway specific responses to anticancer compounds in breast cancer. *Proc Natl Acad Sci U S A* 109(8):2724-2729.
4. Shoemaker RH (2006) The NCI60 human tumour cell line anticancer drug screen. *Nat Rev Cancer* 6(10):813-823.
5. Hafner M, Niepel M, Chung M, & Sorger PK (2016) Growth rate inhibition metrics correct for confounders in measuring sensitivity to cancer drugs. *Nat Methods* 13(6):521-527.
6. Harris LA*, et al.* (2016) An unbiased metric of antiproliferative drug effect in vitro. *Nat Methods* 13(6):497-500.
7. Hsu CH, Altschuler SJ, & Wu LF (2019) Patterns of Early p21 Dynamics Determine Proliferation-Senescence Cell Fate after Chemotherapy. *Cell* 178(2):361-373 e312.
8. Ryl T*, et al.* (2017) Cell-Cycle Position of Single MYC-Driven Cancer Cells Dictates Their Susceptibility to a Chemotherapeutic Drug. *Cell Syst* 5(3):237-250 e238.
9. Tyson DR, Garbett SP, Frick PL, & Quaranta V (2012) Fractional proliferation: a method to deconvolve cell population dynamics from single-cell data. *Nat Methods* 9(9):923-928.
10. Spencer SL*, et al.* (2013) The proliferation-quiescence decision is controlled by a bifurcation in CDK2 activity at mitotic exit. *Cell* 155(2):369-383.
11. Gross SM, Dane MA, Bucher E, & Heiser LM (2019) Individual Cells Can Resolve Variations in Stimulus Intensity along the IGF-PI3K-AKT Signaling Axis. *Cell Syst* 9(6):580-588 e584.
12. Schindelin J*, et al.* (2012) Fiji: an open-source platform for biological-image analysis. *Nat Methods* 9(7):676-682.
13. Berg S*, et al.* (2019) ilastik: interactive machine learning for (bio)image analysis. *Nat Methods* 16(12):1226-1232.
14. McQuin C*, et al.* (2018) CellProfiler 3.0: Next-generation image processing for biology. *PLoS biology* 16(7):e2005970.
15. Meijering E, Dzyubachyk O, & Smal I (2012) Methods for cell and particle tracking. *Methods Enzymol* 504:183-200.

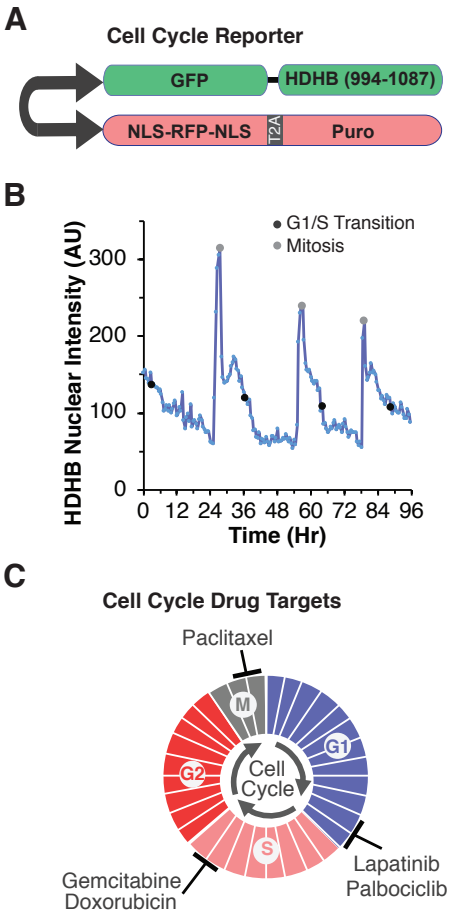

Figure 1. A. Schematic of reporter construct with a bidirectional promoter driving expression of human DNA Helicase B (HDHB) fused to the green fluorescent protein clover, and a second transcript coding for NLS-RFP-NLS, a ribosome skipping domain (T2A), and a puromycin resistance protein. **B.** Quantification of nuclear intensity of the cell cycle reporter in a cell and its progeny across time. The time of G1/S transition and mitosis are demarcated with black and gray circle respectively. **C.** Schematic of the five drugs tested and the cell cycle phase they target.

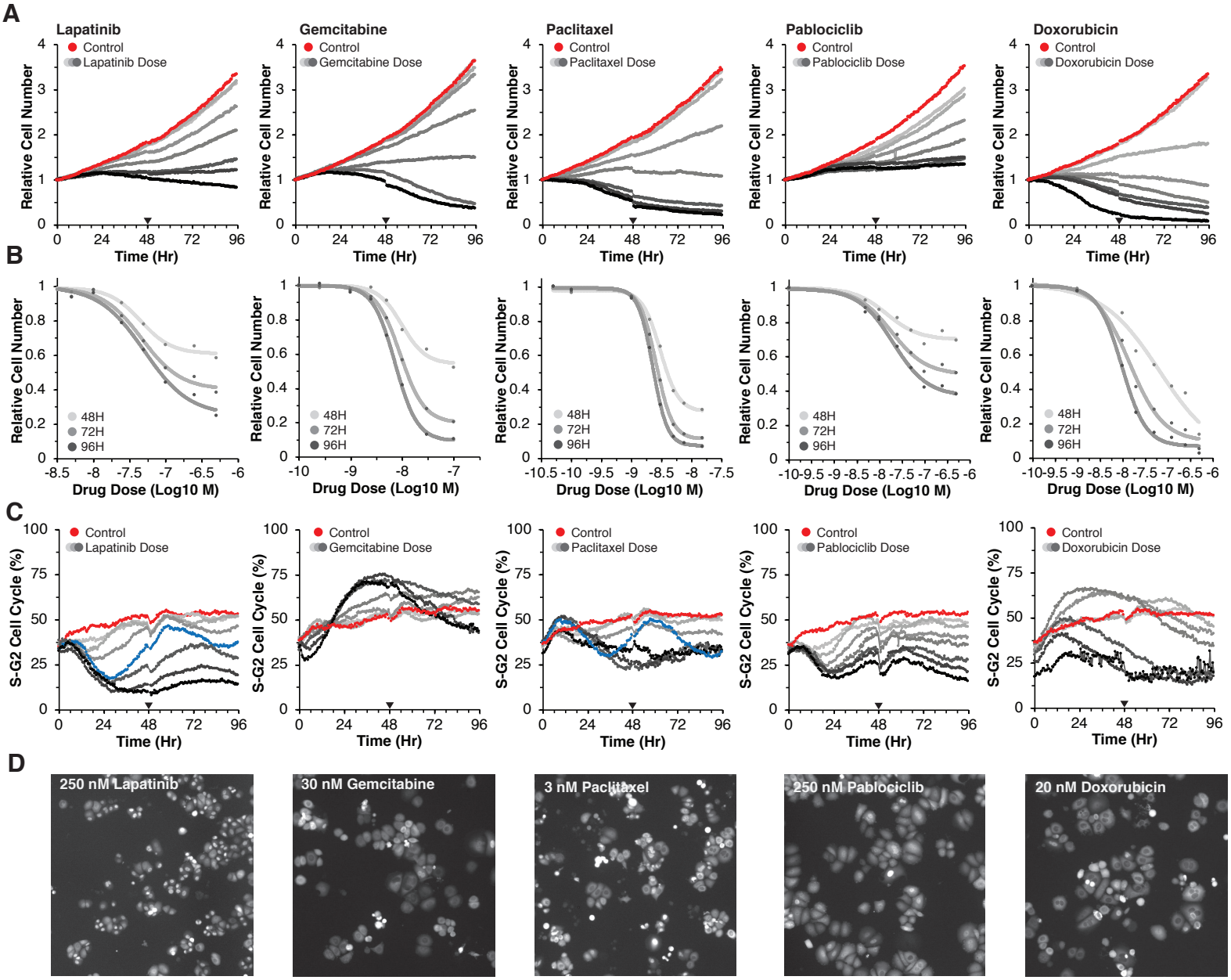

Figure 2. Population responses to drugs vary with dose, time, and cell cycle. A. Average growth curves of AU565 cells tracked every 30 min for 96hr across an 8-point dose response for lapatinib, gemcitabine, paclitaxel, palbociclib, and doxorubicin. The null dose is colored red. Line traces show the average from three independent experiments. The black triangle indicates the addition of fresh drug and media. B. Dose response curves using the relative cell numbers at 48, 72, and 96H. C. Percentage of cells in S/G2 phase of the cell cycle across doses. 50 nM Lapatinib and 3 nM paclitaxel are colored blue. D. GFP images at 39.5H for 250 nM lapatinib, 30 nM gemcitabine, 3 nM paclitaxel, 250 nM palbociclib, 20 nM doxorubicin.

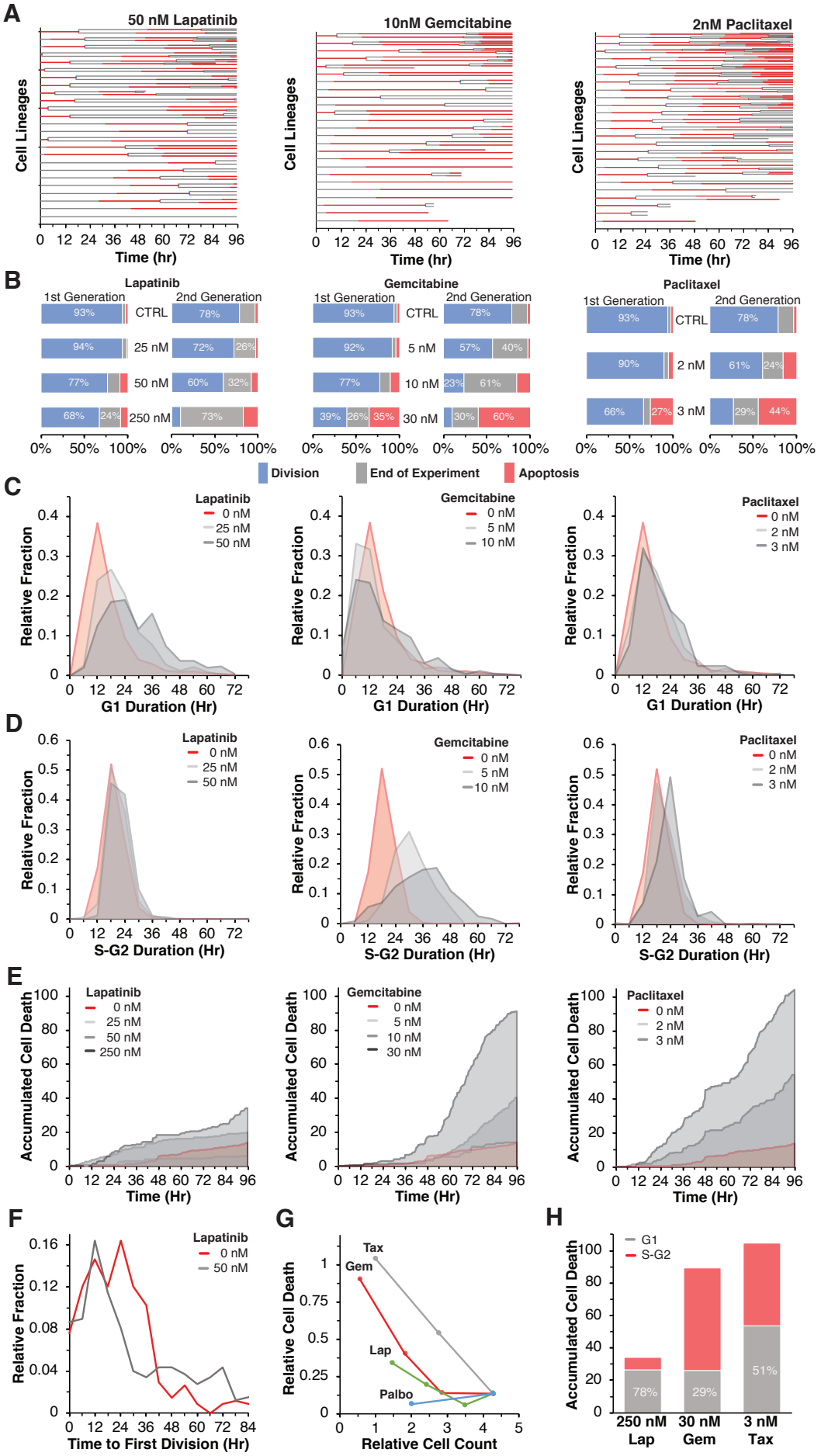

Figure 3. Responses of individual cells reveal molecular mechanisms that vary between drugs. A. Lineage trees for 50nM lapatinib, 10nM gemcitabine, and 2nM paclitaxel showing 25 lineages across 96H. Each track is colored coded based on the cell cycle phase: gray indicates G1 and red indicates S/G2 phase. Track splitting indicates mitosis, and track ending prior to 96H corresponds to apoptosis. B. Quantification of cell outcomes (division, apoptosis, still present at end of experiment) for cells from the first and second generations treated with lapatinib, gemcitabine, or paclitaxel. C. Distributions of G1 durations for cells that had undergone one division. D. Distributions of S-G2 durations. E. Accumulated cell death across time normalized per 100 lineages. F. Time to first division for cells in the CTRL condition (red line) compared to 50 nM lapatinib (gray line). G. Cell count relative to 0H against cell death per lineage. H. Cell death counts per 100 lineages after 96H and the percentage of cells that died in G1 compared to S/G2 for 250nM lapatinib, 30 nM gemcitabine, 3 nM paclitaxel.